Experimental investigation and energy performance simulation of Mongolian Ger with ETS heater and solar PV in Ulaanbaatar city

Bat-Erdene Bayandelger[a,b]*, Yuzuru Ueda[a], and Amarbayar Adiyabat[b]

[a]*Tokyo University of Science, 6 chome-3-1, Niijuku, Katsushika City, Tokyo 123-8585, Japan*
[b]*National University of Mongolia, Ikh sruguuliin gudamj-3, Sukhbaatar district, Ulaanbaatar, 14201, Mongolia*

KEYWORDS

Experimentation
Energy simulation
ETS heater
Mongolian Ger
Solar PV

ABSTRACT

There are ~200.000 households living in the detached houses and ger (yurt) with the small-coal stove which burns a raw coal in the Ulaanbaatar city. The proper heating system and improvement on the energy efficiency of residential dwellings is vital important for Ulaanbaatar city to reduce an air pollution as well as for the operation of current central energy system. This study shows the experimental results of two Gers with two different heating system and different thermal insulation. Technical availability of the system consisting of ETS heater with daytime charging schedule and areal PV system is also examined by using a simulation of MATLAB programming. As a result of the experiment, the indoor comfort level and energy efficiency of the Ger with added insulation and ETS heater with nighttime charging was enhanced to compare with the reference Ger. The Ger with added insulation and ETS heater consumed 3169 kWh for electric appliances and 5989 kWh for the heating season. The simulation was resulted that the ETS heater to be installed in the Ger 2 had prospected to increase the PV self-consumption rate by 76% because of the daytime charging schedule of ETS heater. The PV system supplied 31% of the total energy consumption with remained 69% of the main grid.

1. Introduction

Energy efficient buildings with proper heating system reduces an air pollution, fuel consumption, and electricity costs. In addition, rapidly growing world energy use, climate change is recently demanding the energy-efficient buildings, proper heating system and energy sources [1].

The Ulaanbaatar city is a one of the coldest cities in the world and has a long period of space heating season which continues from annual October to May. ~70% of total energy consumption is used for space heating. There are totally 184,000 households which have a 3-7 kW individual coal burning stoves [2]. Their pollutant emission is recently becoming a biggest problem. ~40% of these households live int the Mongolian ger (yurt). Therefore, improving an energy-efficiency of Mongolian ger and the choice of proper heating system is vital important for reducing a pollutant emission [3] [4]. This paper investigates the energy performance of Mongolian ger with ETS heater and added envelop insulation through the comparative experimentation with reference Ger. Benoit et al., introduced the design and architectural data in his article about the sun clock while Tsovoodavaa et al provided more detailed historical, design, and structural information of the yurt [5] [6]. Also, her extended article presents the results on the thermal dynamic simulations in Mongolian climate [7].

In addition to, the ETS heater play a big role in the integration of renewable energy generation to main grid. Because it has been designed that the electricity converted by heating element to thermal energy is accumulated magnesium brick later use [8] [9] [10] [11] [12]. It also brings various benefits to the customers lowered electricity cost and main grid shifted load and shaved peak [13] [14]. The energy performance of the system which consisting of the 5 kW ETS heater and 3 kWp solar PV to be installed in Ger with added insulation (hereafter referred as the proposed system) is simulated for evaluating potential of the system in this study.

2. Methodology

2.1. Experimentation of the insulated ger with ETS heater

We installed two Mongolian Gers for evaluating the enhancements on energy performance.

Fig. 1 shows a view of installed Gers at Urgakhnaran test site. The Ger shown in Fig. 1 a) has standard envelop materials and coal burning stove (hereafter referred as Ger 1). The Ger in the Fig. 1 b) has added envelop materials and the ETS heater (hereafter referred as Ger 2).

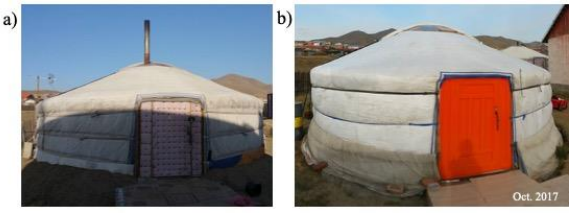

Fig. 1 - (a) the view of Ger 1; (b) Ger 2.

* *Corresponding author*. Tel.: 81-09067456760;
E-mail address: 4317703@ed.tus.ac.jp, e.energy2.0@gmail.com

The thermal and technical details of their envelop materials of these Gers are explained in **Appendix A**. here, the added insulation material on the envelope of Ger 2 is highlighted. The crown wheel of Ger 2 is insulated by 4 mm polycarbonate sheet while 3 mm aluminum foils are aligned through roof, wall, door, door frame and floor for blocking radiation of thermal energy in the Ger 2. We used the 30 mm thicker felt for wall and 100 mm thicker Styrofoam for floor of Ger 2 than Ger 1's. Fig. 2 shows an electrical diagram of experimental setup and electrical wiring of two Gers. As shown in Fig. 2 a), the light, television, refrigerator, and outlet etc., major electrical appliances of Ger 1 is supplied from main grid (1) and total electricity consumption of both Gers are measured by power meter (2) with 3 phase current sensor (3). Voltage (10), current (9), temperature (12), and humidity (11) sensors attached to module loggers of voltage (4), current (5), humidity (6), and temperature (7) measures an electricity consumption, indoor air temperature and humidity. Fig. 2 b) shows an electrical diagram of Ger 2.

Electricity consumption of ETS heater is measured by voltage (4) and current (5) loggers with voltage probe (9) and current clamp (10). The communication base (8) collects all parameters via radio signal. The measurement resolution is 2 min. The measurement continued between 28 October 2017 to 08 June 2018. (refer to **Table 4** of **Appendix B**)

Ger 1 uses a lignite coal for heating and cooking. We measured coal weight just before using in the coal stove. The measurement continued for 20 days in annual coldest month which is January. The lignite coal extracted from the Baganuur coal reserve and the coal weight is converted to kWh unit in according to Kyle's converter [15].

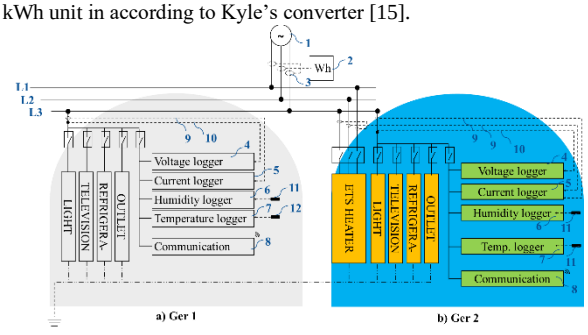

Fig. 2 - Electrical diagram of experimental setup on a) Ger 1 and b) Ger 2.

Table 1 shows an electrical and technical details of the ETS heater installed in Ger 2. The ETS heater has factory equipped with electronically integrated room-temperature control unit and the clock-signal controlled relay. Charging mode of the ETS heater is controlled through the selected charging intensity by customer, and off-peak time of the electricity load in main grid (between 21:00-05:00). For period of the off-peak tariff, K1 relay switches on the thermal relay of the heating element. The charging intensity is set by using 47 $kohm$ potentiometer. If the signal receiving from the core temperature sensor PT100 exceeds a set value of resistance, the temperature regulator disconnects. Maximum value of the core temperature is 460 ^oC. If the room temperature sinks below the set temperature by 47 $kohm$ potentiometer, temperature regulator switches on the heater fan and dissipates warm air into the room and turn of o the set temperature. The 450 $kohm$ resistance regulates a fan speed. Immediate heating demand can provide by day-acting element. Day-acting element run by integrated rocker switch and works on the on-peak tariff.

Table 1 – Electrical and technical detail of the ETS heater

Details	Value
Nominal rating, kW	5
Thermal capacity, kWh	3
Voltage, V	3/N/PE~400
Dimension, mm	850x450x600
Weight, kgs	184

2.2. Simulation of the proposed system

We simulate the operation of solar PV combined with ETS heater for evaluating its energy performance for heating season. The system configuration consists of 5 kW electric heater with 40kWh thermal storage and 3.12 kW PV system. We proposed to use the ETS heater specified at Table 1 in the Ger insulated according to

Appendix A. Envelop elements of Mongolian Ger

Table 3. The electricity generating solar PV system is connected to main grid. The rated nominal capacity of PV array is 3.12 kW and inclined angle of PV array is 45º.

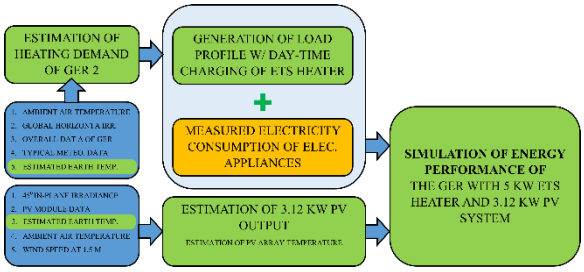

Fig. 3 – The flow chart of energy performance simulation.

The energy performance simulation procedure of ger with ETS heater and solar PV is presented in Fig. 3. Simulation data generally consists of the total electricity consumption, and estimated output of solar PV. Data resolution is 2 min and the data set have same period with the measurement of experimentation. The sum of the electricity consumption of electric appliances and the generated electricity consumption of ETS heater expresses a total electricity consumption. Here, we used the electric consumption of electric appliances in Ger 2 measured from the experimentation. The load profile of ETS heater scheduled to charge at daytime is generated from the estimated daily heating demand of Mongolian ger which has an envelope material specified in **Appendix A**.

The estimation method of heating demand is defined in section 2.3 while section 2.5 details the estimation of solar PV output. (refer to **Table 4** of **Appendix B**)

The electricity flow from the PV system to the main grid can be calculated by subtracting total consumed electricity in the ger from output power of PV system. The amount of electricity consumed in the ger from PV system can be expressed by subtract the electricity flow of PV system to the main grid from output power of PV system. The amount of electricity consumed in the ger from the main grid can be expressed by subtract electricity of PV system consumed in the ger from total consumed electricity in the ger. See the Eq. (1)- (3).

$$P_{grid,t}^{pv} \geq 0, \quad P_{grid,t}^{pv} = P_{pv,t} - P_{ger,t} \tag{1}$$

$$P_{ger,t}^{pv} = P_{pv,t} - P_{grid,t}^{pv} \tag{2}$$

$$P_{grid,t} = P_{ger,t} - P_{ger,t}^{pv} \tag{3}$$

$$Y = \sum_{d=1}^{D} \sum_{t=1}^{T} X_t / D \tag{4}$$

Where, $P_{grid,t}^{pv}$ stands for the electricity flow from solar PV to the main grid at timestep t (kW), $P_{pv,t}$ stands for the electricity generated from the PV system at timestep t (kW), $P_{ger,t}$ stands for the electricity consumed in the ger at timestep t (kW). $P_{ger,t}^{pv}$ is the electricity consumed in the ger from PV system. $P_{grid,t}$ stands for electricity consumed in the ger from the main grid.

Daily amounts of $P_{grid,t}^{pv}$, $P_{ger,t}^{pv}$, and $P_{grid,t}$ were calculated by the sum of 24 hours values. Monthly average daily amounts can be expressed by dividing monthly total value by days per months. See the Eq. (4). Where, X_t stands for the amount of $P_{grid,t}^{pv}$, $P_{ger,t}^{pv}$, and $P_{grid,t}$ at timestep t (kW). T stands for the number of hours per day (24). D stands for the number of days per months. d stands for day number of month.

2.3. Estimation of heating demand

There are various modelling techniques which generally categorized in bottom-up and top-down, are available. Building physics-based modelling is used to estimate a heating demand while. The heating demand of Ger, in another words thermal energy supplying from the ETS heater (H_{ETS}) to Ger, can be expressed by subtracting conduction (H_{Con}), ventilation (H_{Ven}), and infiltration (H_{Inf}) etc., heat losses through building envelope elements and from the heat gains including irradiance (H_{Irr}), occupants (H_{Occ}), and electric appliances (H_{App}). (refer to the Eq (5). The heat loss conducted through walls, doors, crown wheels, ceilings, and floors etc., can be calculated as expressed in Eq. (6). 15% extra heat which is the radiation loss through roofs to space is kept Ger inside by the aluminum foil materials. Since Ger has natural ventilation, Eq. (7) can express the ventilation heat loss whereas the heat loss caused by infiltration can be calculated as shown in Eq. (8).

Where, A is the area of exposed surface (m^2), U is the overall heat transmission coefficient (W/m^2K), $T_{ind,t}$ is the indoor air temperature (20 ^oC). $T_{out,t}$ is the outdoor air temperature at timestep. C_p is the specific heat air (1000 W/kgK), ρ is the density of the air (1.2 kg/m^3). q_v is the air volume flow (m^3/s). n is the number of air replacement in the room per second. V is the room volume (m^3). $n_{adult,t}$ is the number of adults at the timestep, t. $n_{child,t}$ is the number of children at the timestep. $b_{adult,t}$ and $b_{child,t}$ are the binary numbers which expresses an occupied (1) or unoccupied (0). $P_{App,i}$ is the energy rate of the i^{th} electric appliance. $F_{i,t}$ is the heat gain rate of the i^{th} electric appliance (0.734). $b_{i,t}$ is the binary number which indicates either on or off of i^{th} electric appliance. G_{GHI} is the global horizontal irradiance (W/m^2). A_{CW} is a surface area of crown wheel.

Refer to **Table 4**. The measured ambient air temperature is used for estimating the conduction, ventilation, and infiltration heat losses. Heat gain due to irradiance is estimated by using GHI. Physical characteristic data of Mongolian ger and thermal and technical data of it envelop materials are used in the calculations of heat gain and losses.

Estimating a conduction heat loss through floor is not same as the conduction heat loss above ground. The estimation of conduction heat loss through floor involves two significant difficulties including that soil has a specific heat, and so, the heat can both flow and be stored as it flows. Second, the soil temperature changes both with the season and depth from the surface. However, the heat conducted from Ger to the ground ($H_{f,t}$) can be calculated by the following simplified equation (12). The conductance and the earth temperature are modelled in according to Eq. (13) and (14) [16].

$$H_{f,t} = A_f \cdot U_{f,t} \cdot (T_{ind,t} - T_{e,t}) \tag{12}$$

$$U_{f,t} = \frac{0.1140}{4 + R_f} + \frac{0.8768}{16 + R_f} \tag{13}$$

$$T_e = T_{oa,yr} - T_{amp} e^{-D\sqrt{\pi/365\alpha}} cos(\frac{2\pi}{365}(t_{year} - t_{shift} - \frac{D}{2}\sqrt{\frac{365}{\pi\alpha}})) \tag{14}$$

Where, $U_{f,t}$ is effective heat transmission coefficient (W/m^2K). R_f is a thermal resistivity of Ger floor (m^2K/W).

T_e is the effective earth temperature (^oC). $T_{oa,yr}$ is the annual average ambient air temperature (^oC). T_{amp} is the amplitude of the surface temperature (^oC). D is the depth below the surface. α is the thermal diffusivity of the ground soil (10^{-6} m^2/s). t_{year} is the current time. t_{shift} is the day of the year with the minimum surface temperature.

The modelling of the earth temperature uses TMY data. The detail information including the rate of power, time schedule of the occupants, and operation time of major electric appliances are presented in Table 2.

Table 2 – The detail information of the additional heating sources

Details	QTY, pcs	Rate power, W	Weekday schedule	Weekend schedule
Occupants	2 adults &	93	00:00-09:00	00:00-24:00
	2 children	69	18:00-24:00	
Major	1 elect.	1500	07:30–07:50	09:30-09:50
electric	Stove		18:30-18:50	13:30-13:50
appliance				19:30-19:50
Light	1 halo. lamp	50	18:00-23:00	18:00-23:00

2.4. Load profile generation of ETS heater daytime charging

$$H_{ETS,t} = H_{Con,t} + H_{Ven,t} + H_{Inf,t} + H_{Occ,t} + H_{App,t} + H_{Irr,t} \tag{5}$$

$$H_{Con,t} = A \cdot U \cdot (T_{ind,t} - T_{air,t}) \tag{6}$$

$$H_{Ven,t} = C_p \cdot \rho \cdot q_v \cdot (T_{ind,t} - T_{air,t}) \tag{7}$$

$$H_{Con,t} = C_p \cdot \rho \cdot n \cdot V \cdot (T_{ind,t} - T_{air,t}) \tag{8}$$

$$H_{Occ,t} = (n_{adult,t} \cdot b_{adult,t} \cdot P_{child} + n_{child,t} \cdot b_{child,t} \cdot P_{child}) \tag{9}$$

$$H_{App,t} = \sum_{i=1}^{n} b_{i,t} \cdot P_{App,i} \cdot F_{i,t} \tag{10}$$

$$H_{Irr,t} = G_{GHI} \cdot A_{CW} \tag{11}$$

The load profile of Ger with daytime charging of ETS heater is generated for simulating the proposed system. Daily overall heating demand of Ger is calculated from the estimated heating demand with 2 min resolution (refer to Eq. (15). The charging hour per day can be calculated as Eq. (16). The binary number with 2 min interval is created from the calculated charging hour of ETS heater. The ETS charging hours is symmetrically aligned pre and post of midday (12:00 AM). Thus, the ETS heater has an ability to

accumulate the electricity from PV system as much as possible and the PV self-consumption increases. The load profile with the daytime charging can be expressed as multiplication between the created binary numbers and nominal rated power of ETS heater (refer to Eq. (17)).

$$H_{ETS,D} = \sum_{h=1}^{H} \sum_{t=1}^{T} H_{ETS,t} \,/T \quad (15)$$

$$T_{char,h/D} = H_{ETS,D}/P_{ETS,nom} \quad (16)$$

$$P_{ETS\_charging,t} = b_{charge,t} \cdot P_{ETS,nom} \quad (17)$$

Where, T is the number of measurements per hour. $P_{ETS,nom}$ is the nominal rated power of ETS heater. $b_{charge,t}$ is the binary file which indicates on (1) and off (0) of the ETS heater.

2.5. Estimation of solar PV output

Here, we estimate the output power of 3.12 kW solar PV array with 45° inclined angle for simulating the energy performance of proposed system.

The plane of array (POA) irradiance, wind speed, and ambient air temperature of Ulaanbaatar is used to for modelling array temperature and output power of PV. The data resolution is 2 min while data continues from 28 October of 2017 to 08 June of 2018. The Eq. (18) is referred for estimating output power of solar PV.

$$P_{pv,t} = P_{pv,stc} \cdot (G_{POA}/1000) \cdot (1 + \gamma(T_A + 25)) \cdot K \quad (18)$$

$$T_A = G_{POA} \cdot (e^{a+b*WS}) \cdot T_{air} \quad (19)$$

Where, $P_{pv,stc}$ is the rated capacity under Standard Test Condition (STC), γ is the temperature correction coefficient of the maximum power, and K is the loss factor including the incident angle, soil, snow, shading, degradation, conversion, and other unknown losses (0.87). G_{POA} is an irradiance receiving at the 45° inclined plane of array. T_A is the array temperature.

The estimation of array temperature is expressed in the Eq. (19). T_{air} is the ambient air temperature, WS is the wind speed, b and a are parameters that depend on the array construction and materials as well as on mounting configuration of the module (-3.56 and -0.075) [17].

3. Results and discussion

3.1. Experimental results

Fig. 4 shows an indoor heat index of experimented two Gers on the standard heat index. The indoor air temperature of Ger 1 measured in the wider range than the Ger 2 while the humidity of Ger 2 has been increased than the Ger 1 as shown a heat index of Ger 1 and 2 illustrated by black triangles and green triangles.

The fluctuation of wide temperature can be explained through difference between the electronically integrated room temperature control of the ETS heater in Ger 2 and the uncontrolled combustion of coal in the small coal-stove in the Ger 1. Since conduction, ventilation, and infiltration heat gains are direct function of indoor air temperature, the heat consumption also follows the temperature rise. The aluminum foil material could be increased the indoor air humidity of Ger 2. In further, the radiation barrier materials should carefully select for the insulating the Ger.

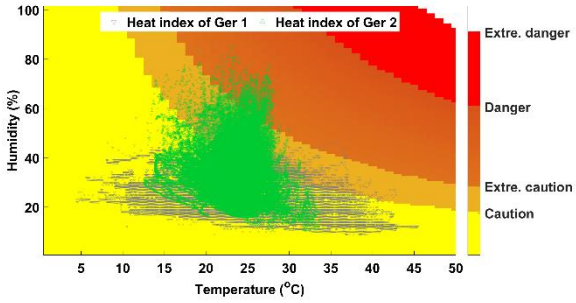

Fig. 4 – The indoor heat indices of experimented two Gers. The black triangular mark indicates the heat index of Ger 1 and the heat index of Ger 2 is presented by the green triangular mark.

Fig. 5 shows a daily energy performance of Ger 1 and 2 at the annual coldest days of year which are January 1 to January 20. The grey and blue colored bar indicates the daily heating consumption and electricity consumption of electric appliances of Ger 1 and the daily energy consumption of Ger 2 is presented by green and aqua colored bars for ETS heater and electric appliances. Here, the ETS heater was set to charge the thermal energy at the nighttime.

The cooking and hot water is supplied by the coal combustion in coal burning stove. Thus, the electricity consumption of the electric appliances in Ger 2 is ~10% higher than Ger 1. On the other side, total heating consumption of Ger 1 is 30% higher than electricity consumption of ETS heater. The added insulation of Ger 2, and electronically integrated room-temperature control unit of the ETS heater etc., could reduce the heating consumption.

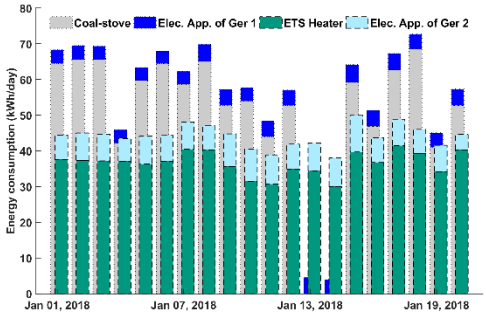

Fig. 5 – Daily energy performances of Ger 1 and 2 at the annual coldest day of year. The grey and blue colored bar indicates the daily heating consumption and electricity consumption of electric appliances of Ger 1 and the daily energy consumption of Ger 2 is presented by green and aqua colored bars for ETS heater and electric appliances.

Ger 1 use 3.88 tn/yr lignite-coal and 0.49 tn/yr wood for space heating and cooking. Whereas, the electric appliances and ETS heater of Ger 2 has been used the 3169 kWh (electric appliances) and 5989 kWh (ETS heater) electricity for period of experimentation.

3.2. Simulation results

Fig. 6 shows a daily operational profile of the Ger with ETS heater and solar PV for one week which is 5th of February to 12th of February. The yellow color indicates the amount of electricity consumed in Ger from PV system. The blue color indicates the amount of electricity consumed in Ger from main grid. The orange color is the electricity flow from PV system to main grid. The amount of electricity from the PV system is sufficiently used in the Ger at the first three days because of availability of solar irradiance while on the 08th and 09th of February, PV self-consumption has a small fraction.

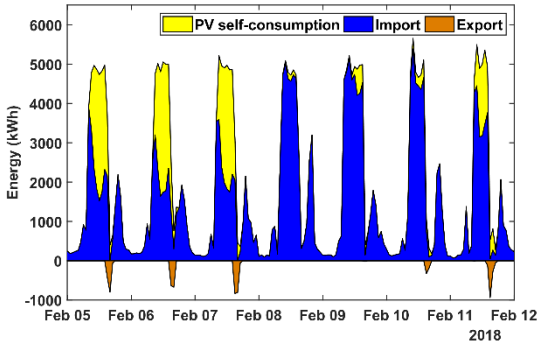

Fig. 6 – The daily operational profile of the Ger with ETS heater and solar PV for one week. The yellow color indicates the amount of electricity consumed in Ger from PV system. The blue color indicates the amount of electricity consumed in Ger from main grid. The orange color is the electricity flow from PV system to main grid.

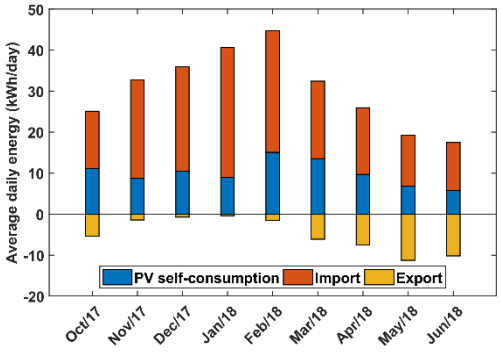

Fig. 7 – Profile of the energy performance of the Ger with ETS heater and solar PV for the heating season. The energy performance is presented by monthly average daily energy consumption. The orange color is the amount of electricity consumed in the Ger from main grid. The blue color is the amount of electricity consumed in Ger from PV system. The yellow color is the electricity flow from PV system to main grid.

Fig. 7 shows a profile of the energy performance of the Ger with ETS heater and solar PV for the heating season. The energy performance is presented by monthly average daily energy consumption. The orange color is the amount of electricity consumed in the Ger from main grid. The blue color is the amount of electricity consumed in Ger from PV system. The yellow color is the electricity flow from PV system to main grid. For period of heating season, the fraction of electricity consumed in the Ger from the solar PV is 31% of the total energy consumption. The remained 69% is the amount of electricity imported from the main grid. The Ger used 76% of the output of PV system while the PV system exported 24% of total output of PV to the main grid.

4. Conclusions

This study experimentally investigated the potential of Ger with ETS heater and added insulation material in cold climate of Ulaanbaatar city by comparing the reference Ger from the viewpoint of energy consumption. In addition to, technical availability of the Ger with ETS heater scheduled to charge during the daytime and solar PV was evaluated by using the simulation based a MATLAB programming script.

The indoor comfort level and energy efficiency of the Ger 2 was enhanced to compare with the Ger 1. In the Ger 2, electric appliances consumed 3169 kWh while 5989 kWh used for the space heating.

The ETS heater installed in the Ger 2 had increased the PV self-consumption rate by 76% because of the daytime charging schedule of ETS heater. The PV system supplied 31% of the total energy consumption with remained 69% of the main grid.

5. Recommendation

- The households living in the detached houses and ger should use the various heater equipped with electronically integrated room-temperature control unit, and the clock-signal controlled relay. Because they allow an energy saving for space heating and effectively interact with the CES.

6. In connections to further study

- The potential for supplying a demand of hot water through the surplus power of solar PV has prospected when there is no heating demand in summer. Therefore, various type of thermal storages materials, for instance water, ceramic, and phase change material (PCM), are needed to be considered in the system configuration of this study.
- Optimal operation of ETS heater powered by the solar PV in main grid has an availability to reduce electricity cost for customers, increase renewable energy installation in main grid.

Acknowledgement

Authors would like to acknowledge the Mongolian-Japan Engineering Education Development (MJEED) program.

Bibliography

[1] J. Conti, P. Holtberg, J. Diefenderfer, A. LaRose, J. T. Turnure and L. Westfall, "International energy outlook 2016 with projections to 2040," USDOE Energy Information Administration (EIA), Washington, DC, 2016.

[2] "Mongolian Statistical Information Service," National Statistics Office, [Online]. Available: www.1212.mn.

[3] D. Perry K, G. Gerelmaa, M. Andreas, T. William J, B. Bernard J, D. Shagjjambe and L. Sereeter, "Air particulate matter pollution in Ulaanbaatar, Mongolia: determination of composition, source contributions and source locations," *Atmospheric Pollution Research*, vol. 2, no. 2, pp. 126-137, 2011.

[4] G. Sarath K, S. Lodoysamba, B. Bulgansaikhan and B. Dashdondog, "Particulate pollution in Ulaanbaatar, Mongolia," *Air Quality, Atmosphere & Health*, vol. 6, no. 3, pp. 589-601, 2013.

[5] T. Gantumur, S. Rowell Ray Lim, M. R. Ganjali and I. Kistelegdi, "A review and systemization of the traditional Mongolian yurt (GER)," *Pollack Periodica*, vol. 13, no. 3, pp. 19--30, 2018.

[6] B. Mauvieux, R. Alain and T. Yvan, "The yurt: A mobile home of nomadic populations dwelling in the Mongolian steppe is still used both as a sun clock and a calendar," vol. 31, no. 2, pp. 151--156, 2014.

[7] T. Gantumur and I. Kistelegdi, "Comparative analysis for traditional yurts using thermal dynamic simulations in Mongolian climate," *Pollack Periodica*, vol. 14, no. 2, pp. 97-108, 2019.

[8] C. H. W, H. R. Stephen and M. T. Sulatisky, "Thermal energy storage in forced-air electric furnaces," *IEEE Transactions on Industry Applications*, no. 1, pp. 127--133, 1980.

[9] V. G. Miriam, "Electric thermal-storage heaters," *Electronics and Power*, vol. 10, no. 3, pp. 68--71, 1964.

[10] W. R. Coleman and C. M. Grastataro, "American electric power system electric thermal storage program: An evaluation of performance within the home," *IEEE Transactions on Power Apparatus and Systems*, no. 12, pp. 4741--4749, 1981.

[11] B. Y. Bedouani, A. Moreau, M. Parent and L. Blaise, "Central electric thermal storage (ETS) feasibility for residential applications: Part 1. Numerical and experimental study," *International journal of energy research*, vol. 25, no. 1, pp. 53--72, 2001.

[12] B. Y. Bedouani, B. Labreque, M. Parent and A. Legault, "Central electric thermal storage (ETS) feasibility for residential applications: Part 2. Techno-economic study," *International journal of energy research*, vol. 25, no. 1, pp. 73--83, 2001.

[13] W. Steven and J.-P. Pinard, "Opportunities for smart electric thermal storage on electric grids with renewable energy," *IEEE Transactions on Smart Grid*, vol. 8, no. 2, pp. 1014-1022, 2016.

[14] S. Patrick S, S. Bharatkumar V, C. Claudio A and K. Hohman Soren, "Electric thermal storage system impact on northern communities' microgrids," *IEEE Transactions on Smart Grid*, vol. 10, no. 1, pp. 852--863, 2017.

[15] "kylesconverter," [Online]. Available: http://www.kylesconverter.com/.

[16] K. Tamami and A. Paul R, "Earth temperature and thermal diffusivity at selected stations in the United States," National Bureau of Standards, 1965.

[17] A. Luketa-Hanlin and J. Stein, "IMPROVEMENT AND VALIDATION OF A TRANSIENT MODEL TO PREDICT PHOTOVOLTAIC MODULE TEMPERATURE," in *World Renewable Energy Forum*, Denver, 2012.

[18] K. M, A. Mavrogianni, D. Mumovic, S. A, S. Z and D.-P. M, "A review of bottom-up building stock models for energy consumption in the residential sector," *Building and environment*, vol. 45, no. 7, pp. 1683--1697, 2010.

* *Corresponding author*. Tel.: 81-09067456760;
E-mail address: 4317703@ed.tus.ac.jp, e.energy2.0@gmail.com

Appendix A. Envelop elements of Mongolian Ger

Table 3 - The thermal and technical description of envelope materials used in Ger 1 and 2.

№		Description of Ger 1's envelope elements	Description of Ger 2's envelope elements
1	Crown wheel	Layer 1: 150 mm wooden frame with 0.17 $W/k \cdot m$ ther. cond. Layer 2: 50 mm felt with 0.04 $W/k \cdot m$ thermal conductivity Layer 3: 3 mm glass with 0.8 $W/k \cdot m$ thermal conductivity	Layer 1: 150 mm wooden frame with 0.17 $W/k \cdot m$ thermal cond. Layer 2: 50 mm felt with 0.04 $W/k \cdot m$ thermal conductivity Layer 3: 3 mm glass with 0.8 $W/k \cdot m$ thermal conductivity **Layer 4: 4 mm polycarbonate sheet**
2	Roof	Layer 1: Φ30 mm wooden pole with 0.17 $W/k \cdot m$ ther. cond. Layer 2: 2 mm linen with 0.04 $W/k \cdot m$ thermal conductivity Layer 3: 50 mm felt with 0.04 $W/k \cdot m$ thermal conductivity Layer 4: 2 mm linen with 0.04 $W/k \cdot m$ thermal conductivity	Layer 1: Φ30 mm wooden pole with 0.17 $W/k \cdot m$ thermal cond. Layer 2: 2 mm linen with 0.04 $W/k \cdot m$ thermal conductivity Layer 3: 50 mm felt with 0.04 $W/k \cdot m$ thermal conductivity Layer 4: 2 mm linen with 0.04 $W/k \cdot m$ thermal conductivity **Layer 5: 3 mm alum. foil with 0.04 $W/k \cdot m$ thermal cond.**
3	Wall	Layer 1: 2 mm linen with 0.04 $W/k \cdot m$ thermal conductivity Layer 2: 14 mm wooden lattice with 0.17 $W/k \cdot m$ therm. cond. Layer 3: 2 mm linen with 0.04 $W/k \cdot m$ thermal conductivity Layer 4: 50 mm felt with 0.04 $W/k \cdot m$ thermal conductivity Layer 5: 2 mm linen with 0.04 $W/k \cdot m$ thermal conductivity	Layer 1: 2 mm linen with 0.04 $W/k \cdot m$ thermal conductivity Layer 2: 14 mm wooden lattice with 0.17 $W/k \cdot m$ thermal cond. Layer 3: 2 mm linen with 0.04 $W/k \cdot m$ thermal conductivity **Layer 4: 80 mm felt with 0.04 $W/k \cdot m$ thermal conductivity** Layer 5: 2 mm linen with 0.04 $W/k \cdot m$ thermal conductivity **Layer 6: 3 mm alum. foil with 0.04 $W/k \cdot m$ thermal cond.**
4	Door	Layer 1: 20 mm wood with 0.17 $W/k \cdot m$ thermal cond. Layer 2: 20 mm felt with 0.04 $W/k \cdot m$ thermal conductivity	Layer 1: 20 mm wood with 0.17 $W/k \cdot m$ thermal cond. Layer 2: 20 mm felt with 0.04 $W/k \cdot m$ thermal conductivity **Layer 3: 3 mm alum. foil with 0.04 $W/k \cdot m$ thermal cond.**
5	Door frame	Layer 1: 30 mm wood with 0.17 $W/k \cdot m$ thermal cond. Layer 2: 40 mm felt with 0.04 $W/k \cdot m$ thermal conductivity	Layer 1: 30 mm wood with 0.17 $W/k \cdot m$ thermal cond. Layer 2: 40 mm felt with 0.04 $W/k \cdot m$ thermal conductivity **Layer 3: 3 mm alum. foil with 0.04 $W/k \cdot m$ thermal cond.**
6	Floor	Layer 1: 20 mm wood with 0.17 $W/k \cdot m$ thermal cond. Layer 2: 50 mm Styrofoam with 0.03 $W/k \cdot m$ thermal cond.	Layer 1: 20 mm wood with 0.17 $W/k \cdot m$ thermal cond. Layer 2: **150 mm** Styrofoam with 0.03 $W/k \cdot m$ thermal cond. **Layer 3: 3 mm alum. foil with 0.04 $W/k \cdot m$ thermal cond.**

Appendix B. The data description

Table 4 - The description of data.

№	Parameters	Period	Resolution	Application of data			
				Experimental Investigation	Estimation of heating demand	Estimation of solar PV output	Simulation of Proposed System
	1. Wireless communication base modular logger						
1.1	Indoor air temperature of Ger 1, (^{o}C)	28/Oct/17 – 08/Jun/18	2 min	+			
1.2	Indoor air humidity of Ger 1, (%)	28/Oct/17 – 08/Jun/18	2 min	+			
1.3	Consumption of major elec. App. of Ger 1, (kW)	28/Oct/17 – 08/Jun/18	2 min	+			
1.4	Coal weight, (kg)	01/Jan/18 – 20/Jan/18	3 hours	+			
1.5	Indoor air temperature of Ger 2, (^{o}C)	28/Oct/17 – 08/Jun/18	2 min	+			
1.6	Indoor air humidity of Ger 2, (%)	28/Oct/17 – 08/Jun/18	2 min	+			
1.7	Consumption of major elec. App. of Ger 2, (kW)	28/Oct/17 – 08/Jun/18	2 min	+			+
1.8	Consumption of ETS heater, (kW)	28/Oct/17 – 08/Jun/18	2 min	+			
	2. Meteorological weather station data						
2.1	Outdoor air temperature, (^{o}C)	28/Oct/17 – 08/Jun/18	2 min	+	+	+	
2.2	Outdoor air humidity, (%)	28/Oct/17 – 08/Jun/18	2 min				
2.3	Global horizontal irradiance, (kW/m^2)	28/Oct/17 – 08/Jun/18	2 min		+		
2.4	45° plane of array irradiance, (kW/m^2)	28/Oct/17 – 08/Jun/18	2 min			+	
2.5	Wind speed, (m/s)	28/Oct/17 – 08/Jun/18	2 min			+	
	3. Other data						
3.1	Typical Meteorological Year (TMY) Data				+		
3.2	Physical characteristic data of Ger				+		
3.3	Thermal and technical data of Ger's envelop materials			+	+		
	4. Composed and estimated data						
4.1	Estimated earth temperature, T_e	28/Oct/17 – 08/Jun/18	2 min		+		
4.2	Binary number of adult occupations	28/Oct/17 – 08/Jun/18	2 min		+		+
4.2	Binary number of child occupation	28/Oct/17 – 08/Jun/18	2 min		+		
4.3	Binary number of elec. Application operation,	28/Oct/17 – 08/Jun/18	2 min		+		
4.4	Estimated heating demand	28/Oct/17 – 08/Jun/18	2 min				+
	Binary numbers of the ETS heater operation	28/Oct/17 – 08/Jun/18	2 min				+
4.5	Generated load profile of daily heating demand	28/Oct/17 – 08/Jun/18	2 min				+
4.6	Estimated output power solar PV	28/Oct/17 – 08/Jun/18	2 min				+

Appendix C. The validation of the estimated heating demand and solar PV output

Table 5 - The MAPE, MAE, and RMSE of estimated heating demand and PV output

Year	Estimated heating demand			Estimated PV output		
	MAPE, %	**MBE, kWh**	**RMSE, kWh**	**MAPE, %**	**MBE, kWh**	**RMSE, kWh**
2017/10	17.96	3.58	1.52	5.38	1.00	0.985
2017/11	13.31	4.17	2.23	16.13	2.15	1.26
2017/12	11.98	3.99	2.33	23.94	1.84	0.51
2018/01	5.54	2.02	0.36	9.78	0.80	0.54
2018/02	3.83	1.26	0.91	6.26	1.06	0.42
2018/03	24	5.21	3.47	3.40	0.51	0.51
2018/04				23.40	3.58	3.45
2018/05				2.6	0.56	0.57
2018/06						